Electronic Supplementary Information

Graphene oxide and gold nanoparticle based nanocomposite for aptamer-based electrochemical detection of CD36

Simge Er Zeybekler*[a], Sultan Sacide Gelen[a], Togzhan Akhmetova[a], Dilek Odaci[a]

[a]Faculty of Science Biochemistry Department, Ege University, Bornova, Izmir, 35100, Türkiye. E-mail: simge.er.zeybekler@mail.ege.edu.tr

Table of Contents

Section A. Materials and Methods

Materials

Graphite powder (GR, <20 μm, synthetic), concentrated sulfuric acid (H_2SO_4) 95.0–98.0% (w/w), phosphoric acid (H_3PO_4) 85% (w/w), $KMnO_4$ (99%), H_2O_2 solution (30%), 4-aminothiophenol (4ATP), sodium nitrite ($NaNO_2$), urea (99.0–100.5 %), bovine serum albumin (BSA, ≥98.0 %), insulin (INS), D-glucose (GLC, ≥99.5 %), potassium chloride (KCl),potassium phosphate monobasic (KH_2PO_4), sodium sulfate decahydrate ($Na_2SO_4 \cdot 10H_2O$), sodium chloride (NaCl), human serum (H4522), tetrachloroauric(III) acid trihydrate ($HAuCl_4 \cdot 3H_2O$), trisodium citrate, potassium, magnesium chloride ($MgCl_2$), Tris hydrochloride (TRIS-HCl), potassium hexacyanoferrate (III) (HCF, $K_3[Fe(CN)_6]$) were purchased from Sigma-Aldrich (Germany). The CD36 aptamer (1 μmol) with the sequence 5′-Amino-C6-CGACACCTCCAGACGCACGCTCGACACGACACCTCCAGACCGCCTCGTCCACTGTGCCTC-Thiol (SH)-3′ was purchased from Ella Biotech GmbH (Fürstenfeldbruck, Germany) and used without further purification.[1] CD36 aptamer and CD36 standard solutions were prepared in a 10 mM Tris–HCl buffer (pH 7.4) supplemented with 100 mM NaCl and 5 mM $MgCl_2$.

Apparatus

The structural and surface properties of the materials were analyzed by SEM–EDS (Thermo Scientific Apreo S) and ATR–FTIR (PerkinElmer Spectrum Two, USA) within the 4000–600 cm^{-1} spectral region. Electrochemical experiments were conducted using a PalmSens4 potentiostat (Palm Instruments, Houten, Netherlands) combined with a screen-printed carbon electrode (SPCE, C110, 4 mm diameter). The electrode system included an integrated Ag pseudo-electrode and a carbon counter electrode (Metrohm, Switzerland). The SPCE was connected to the potentiostat through a 4 mm banana-type SPE connector.

Synthesis of GO-4ATP/AuNPs

GO was synthesized from GR using a modified Hummers' method.[2] In brief, 1.0 g of GR and 6.0 g of $KMnO_4$ were dispersed in a mixture of H_2SO_4 and H_3PO_4 (9:1, v/v) and stirred at 50 °C for 12 h. The reaction mixture was then poured onto ice (130 mL of frozen distilled water), followed by the addition of 1 mL of 30% (w/v) H_2O_2. The resulting suspension was centrifuged at 4000 rpm for 4 h. The obtained GO was washed sequentially with 10% (w/v) HCl solution and ethanol to remove residual metal ions, and finally dried at 60 °C overnight.

To obtain GO–4ATP, a 0.05 M 4ATP solution was prepared in 0.5 M HCl. Subsequently, an equimolar amount of $NaNO_2$ was added under ice–water bath conditions to generate the corresponding diazonium intermediate. Separately, GO was dispersed in ultrapure water by sonication for 30 min and then introduced into the 4ATP–$NaNO_2$ solution at a final concentration of 1 mg/mL. The reaction mixture was stirred for 24 h under ice-bath conditions. After completion, the product was collected by centrifugation at 13,000 rpm and thoroughly washed with acetone, ethanol, and deionized water. The resulting GO–4ATP was then dried in an oven at 60 °C for 24 h.[3-5]

To prepare the GO-4ATP/AuNPs nanocomposite, 4 mg of GO was dispersed in 50 mL of deionized water and stirred at room temperature for 1 h. Subsequently, 15 mg of $HAuCl_4 \cdot 3H_2O$ was introduced into the suspension, followed by incubation for 30 min to facilitate the interaction between Au^{3+} ions and the GO surface. Thereafter, 5 mL of sodium citrate solution (sodium citrate/deionized water mass ratio: 0.02) was added dropwise under continuous stirring, and the mixture was further stirred for 30 min. The reaction mixture was then heated to 80 °C and maintained at this temperature for 1 h. After completion of the reaction, the resulting nanocomposite was washed three times with distilled water and centrifuged at 7000 rpm to eliminate unreacted AuNPs. Finally, the obtained AuNP/4ATP/GO nanocomposite was dried at 60 °C for 12 h.[6]

Preparation of Aptamer-Functionalized Electrodes (GO-4ATP/AuNPs/CD36APT/SPCE)

The SPCE working electrode was coated with GO–4ATP/AuNPs nanocomposite via drop-casting. An aliquot (4 µL) of the nanocomposite suspension (3 mg/mL) was applied to the electrode surface and dried at ambient conditions for 30 min. The electrodes were then washed with deionized water and dried before CD36APT immobilization.

The CD36 aptamer solution (2.5 µM) was prepared in 10 mM Tris–HCl buffer (pH 7.4) supplemented with 100 mM NaCl and 5 mM $MgCl_2$ to ensure proper folding and structural stability. Prior to immobilization, the aptamer solution was thermally treated at 95 °C for 5 min, followed by cooling to room temperature. The aptamer solution was then drop-cast onto the GO-4ATP/AuNPs-modified SPCE surface and incubated at 4 °C for 1 h to minimize solution evaporation and ensure efficient integration of the aptamer with the nanomaterial-modified electrode surface.[7, 8] The electrodes were subsequently rinsed with deionized water and dried prior to electrochemical measurements. CD36 incubation and subsequent detection experiments were performed at room temperature.

Electrochemical measurements

Electrochemical measurements were carried out using a SPCE coupled to a PalmSens4 potentiostat controlled by PSTrace 5.12 software. All experiments were performed at ambient temperature (25.0±0.5 °C). Cyclic voltammetry (CV) and differential pulse voltammetry (DPV) were conducted at a scan rate of 50 mV/s over a potential window of −0.4 to +0.8 V. Electrochemical impedance spectroscopy (EIS) measurements were recorded over a frequency range of 0.018 Hz-1 kHz using an AC amplitude of 0.18 V. The electrochemical experiments were performed in 10 mM PBS (pH 7.4) containing 5.0 mM hexacyanoferrate (HCF) as the redox probe and 0.1 M KCl.

Section B. Characterization of GO-4ATP/AuNPs

TEM images at different magnifications reveal the morphology of the GO-4ATP/AuNPs nanocomposite and show electron-dense nanoparticulate structures within the GO matrix. Furthermore, Au elemental mapping confirms the distribution of Au within the nanocomposite, while EDS analysis verifies the presence of Au (12.85 wt%) together with C, N, O, and S elements. These additional TEM, elemental mapping, and EDS results provide direct evidence for the successful incorporation and distribution of AuNPs within the GO–4ATP framework (Fig. S1).

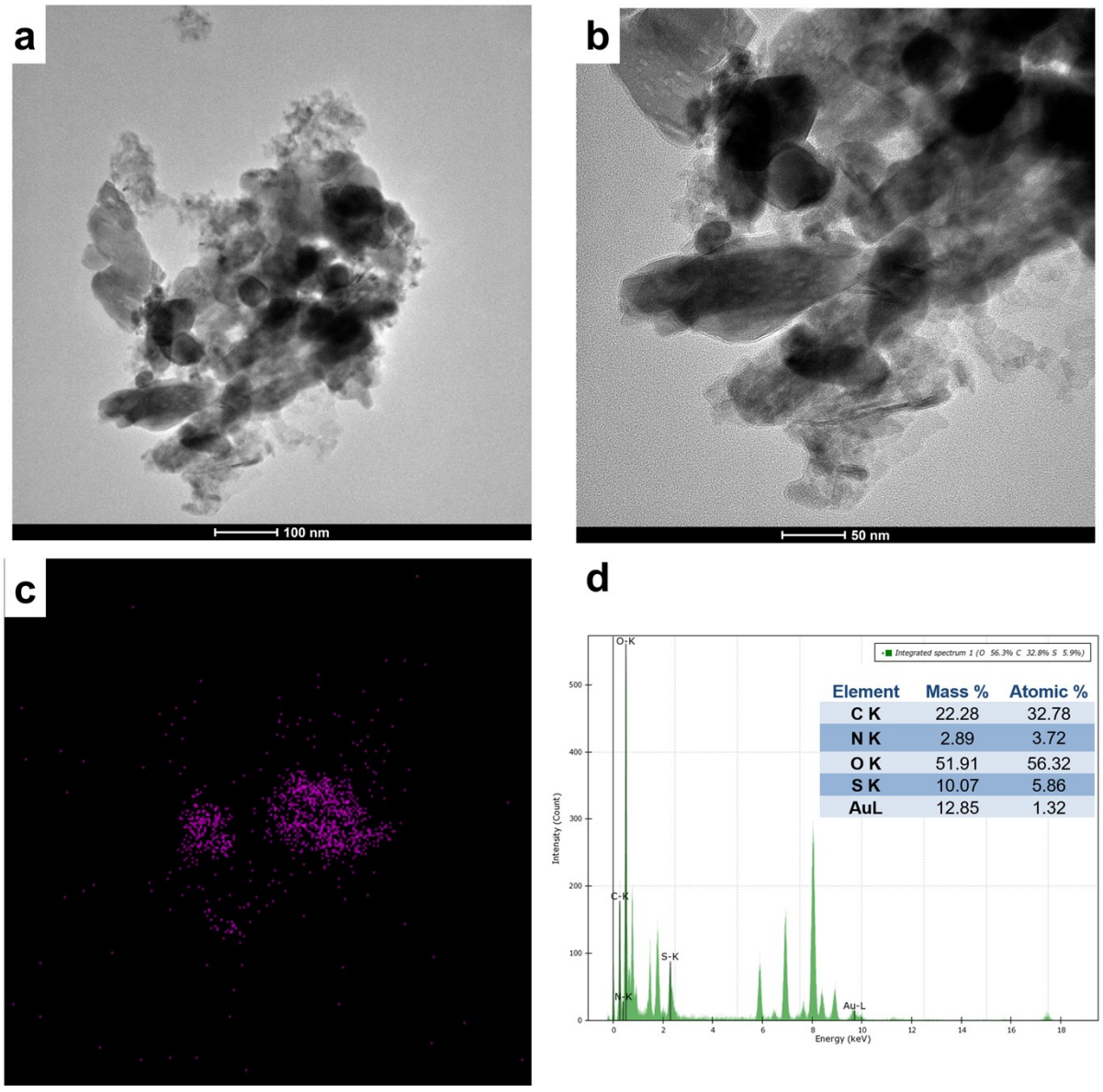

Fig. S1. TEM/STEM characterization of the GO-4ATP/AuNPs nanocomposite. (a,b) TEM images recorded at different magnifications showing the morphology of the GO–4ATP/AuNPs nanocomposite; scale bars: 100 nm in (a) and 50 nm in (b), (c) Au elemental mapping demonstrating the distribution of Au within the nanocomposite, (d) EDS spectrum and elemental composition of the GO–4ATP/AuNPs nanocomposite.

Section C. Electrochemical characterization

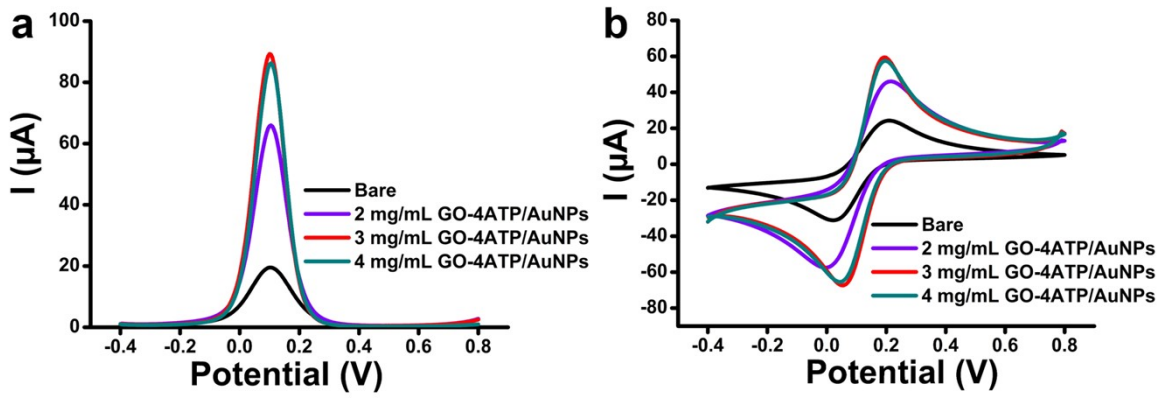

Fig. S2. (a) DPV profiles of bare SPCE and SPCE modified with GO–4ATP/AuNPs nanocomposite at different concentrations, (b) CV profiles of bare SPCE and SPCE modified with GO–4ATP/AuNPs nanocomposite at different concentrations. (All measurements were conducted in 10 mM PBS at pH 7.4, supplemented with 5.0 mM HCF and 0.1 M KCl. The scan rate employed for the analysis was 50 mV/s).

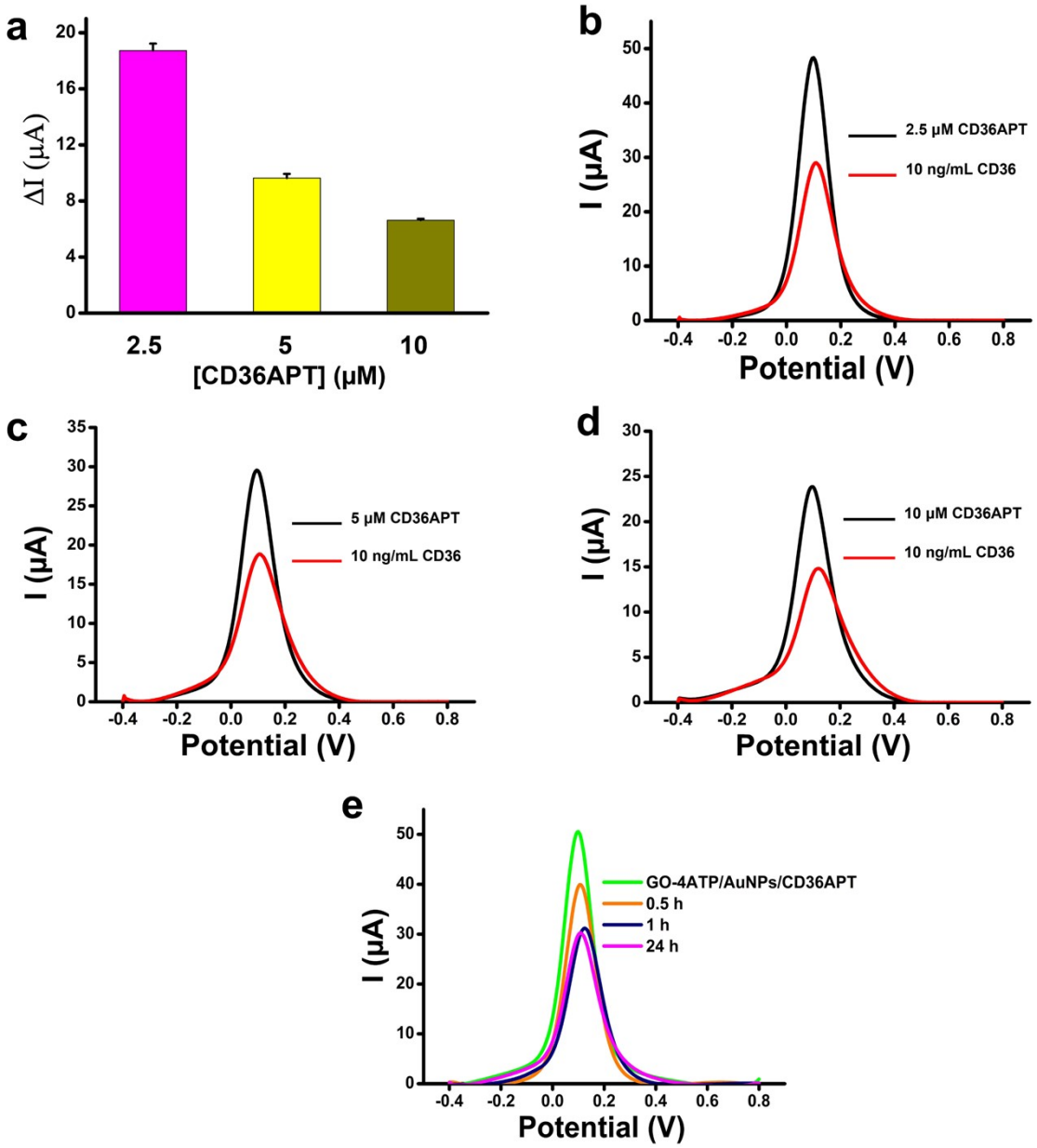

Fig. S3. Optimization of the aptamer immobilization conditions for the GO–4ATP/AuNPs/CD36APT aptasensor. (a) Effect of CD36APT concentration on the current change (ΔI) in the presence of 10 ng/mL CD36. DPV responses obtained from GO-4ATP/AuNPs/CD36APT-modified SPCEs prepared with different aptamer concentrations: (b) 2.5 μM CD36APT, (c) 5 μM CD36APT, and (d) 10 μM CD36APT in the absence and presence of 10 ng/mL CD36. (e) Effect of aptamer immobilization time (0.5, 1, and 24 h) on the DPV response of the GO-4ATP/AuNPs/CD36APT-modified SPCE. (All measurements were performed in 10 mM PBS (pH 7.4) containing 5.0 mM HCF and 0.1 M KCl. Data are presented as mean ± SD (n = 3)).

The electroactive surface area of the GO-4ATP/AuNPs-modified SPCE was estimated using the Randles–Sevcik equation:

$$I_p = (2.69 \times 10^5) n^{3/2} D^{1/2} C A v^{1/2} \quad \text{(Eq. S1)}$$

where I_p is the peak current (Ampere), n is the number of transferred electrons (equal to 1), A is the electroactive surface area (cm^2), D is the diffusion coefficient of the redox probe (for $K_3[Fe(CN)_6]$ is 7.6×10^{-6} cm^2/s), C is the concentration of $K_3[Fe(CN)_6]$ (mol/cm^3), and v is the scan rate (V/s).[9, 10]

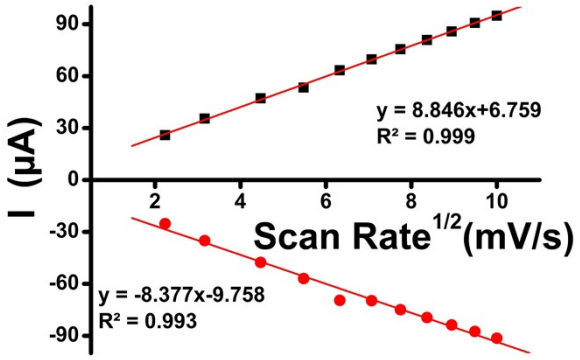

Fig. S4. Linear relationship between anodic and cathodic peak currents and the square root of scan rate.

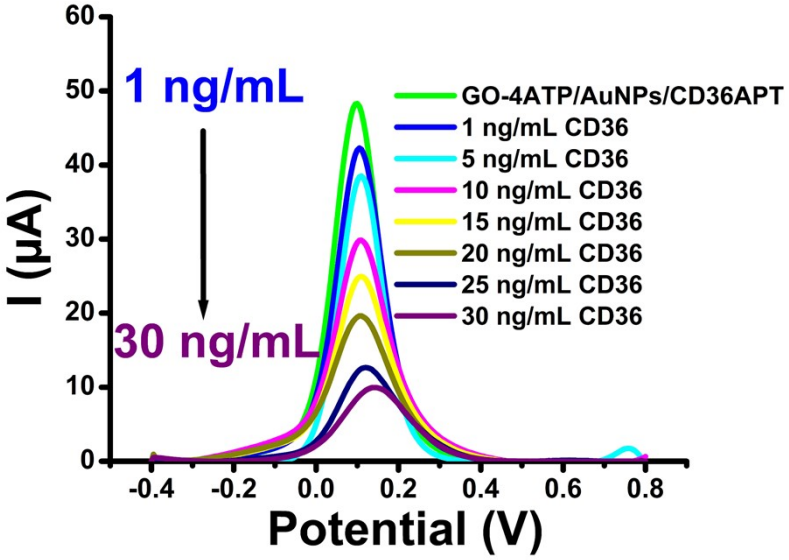

Fig. S5. DPV profiles recorded at increasing CD36 concentrations.

As summarized in Table S1, only a limited number of electrochemical biosensors have been reported for CD36 detection, and aptamer-based platforms remain particularly scarce. Most previously reported CD36 sensors rely on antibodies as recognition elements, which are associated with relatively high production costs, batch-to-batch variability, and limited storage stability. In contrast, aptamers offer advantages including lower production cost, improved chemical stability, and facile surface modification. Although a recently reported Au@MoS_2 CD36 aptasensor exhibited a lower detection limit, it was primarily developed for the detection of CD36-expressing breast cancer-derived exosomes. In contrast, the present GO-4ATP/AuNPs/CD36APT platform was designed for the direct determination of soluble CD36 protein in serum samples, while maintaining competitive analytical performance. These findings demonstrate the potential of the proposed aptasensor as a cost-effective and reliable alternative to antibody-based CD36 sensing platforms.

Table S1. Comparison of the analytical performance of the proposed GO-4ATP/AuNPs/CD36APT aptasensor with previously reported electrochemical biosensors for CD36 detection.

Sensor Platform	**Recognition Element**	**Linear Range**	**LOD**	**Ref.**
PS/MWCNT-PAMAM ENs	Anti-CD36	5–40 ng/mL	3.94 ng/mL	[11]
PS/GO-APTES ENs	Anti-CD36	0.5–20 ng/mL	0.999 ng/mL	[12]
Au@MoS_2	CD36 APT	0.1-10^8 pM	0.4 pM	[13]
GO-4ATP/AuNPs	CD36 APT	1–30 ng/mL	0.45 ng/mL	This study
PS/MWCNT-PAMAM ENs; polystyrene/multiwall carbon nanotube-polyamidoamine electrospun nanofibers; PS/GO-APTES ENs: polystyrene/graphene oxide-(3-aminopropyl)triethoxysilane electrospun nanofibers; Au@MoS_2: gold-decorated molybdenum disulfide.				

References

1. Y. Pu, J. Xiang, X. Zhang, Y. Deng, H. Liu and W. Tan, *Analytical Chemistry*, 2021, **93**, 3951-3958.
2. D. C. Marcano, D. V. Kosynkin, J. M. Berlin, A. Sinitskii, Z. Sun, A. S. Slesarev, L. B. Alemany, W. Lu and J. M. Tour, *ACS Nano*, 2018, **12**, 2078-2078.
3. A. A. Ensafi, M. Jafari-Asl and B. Rezaei, *Journal of Electroanalytical Chemistry*, 2014, **731**, 20-27.
4. D. Chen, H. Zhang, K. Yang and H. Wang, *Journal of Hazardous Materials*, 2016, **310**, 179-187.
5. P. Mirzaei, S. Bastide, A. Aghajani, J. Bourgon, É. Leroy, J. Zhang, Y. Snoussi, A. Bensghaier, O. Hamouma, M. M. Chehimi and C. Cachet-Vivier, *Langmuir*, 2019, **35**, 14428-14436.
6. J. Song, L. Xu, R. Xing, Q. Li, C. Zhou, D. Liu and H. Song, *Scientific reports*, 2014, **4**, 7515.
7. A. Villalonga, C. Parrado, R. Díaz, A. Sánchez, B. Mayol, P. Martínez-Ruíz, D. Vilela and R. Villalonga, *Biosensors*, 2022, **12**, 514.
8. S. Pushparajah, M. Shafiei and A. Yu, *Biosensors*, 2025, **15**, 15.
9. S. Er Zeybekler, D. Odaci and N. Horzum, *Microchemical Journal*, 2025, **209**, 112811.
10. M. G. Trachioti, A. C. Lazanas and M. I. Prodromidis, *Microchimica Acta*, 2023, **190**, 251.
11. S. Er Zeybekler and D. Odaci, *ACS Omega*, 2023, **8**, 5776-5786.
12. S. Er and D. Odaci Demirkol, *Bioelectrochemistry*, 2022, **145**, 108083.
13. M. Lee, Y. Han, H. Park, D. Yoo, H. Y. Yoo, J.-H. Lee and T. Lee, *Bioelectrochemistry*, 2026, **170**, 109247.